Blocking chondrocyte hypertrophy in conditional *Evc* knockout mice does not modify osteoarthritis progression

Ana Lamuedra[1], Paula Gratal[1], Lucía Calatrava[2,3], Víctor Luis Ruiz-Perez[2,3,4], Adrián Palencia-Campos[2], Sergio Portal-Núñez[5], Aránzazu Mediero[1], Gabriel Herrero-Beaumont[1], Raquel Largo[1]

[1]Bone and Joint Research Unit, Service of Rheumatology, IIS-Fundación Jiménez Díaz, Autonomous University of Madrid, 28040 Madrid, Spain

[2]Instituto de Investigaciones Biomédicas 'Alberto Sols', CSIC-UAM, 28029 Madrid, Spain

[3]CIBER de Enfermedades Raras (CIBERER), ISCIII, Spain

[4]Instituto de Genética Médica y Molecular (INGEMM), Hospital Universitario La Paz-IdiPaz-UAM, 28046 Madrid, Spain

[5]Bone Physiopathology Laboratory, Applied Molecular Medicine Institute (IMMA), Universidad San Pablo-CEU, CEU 6 Universities, Campus Monteprincipe, 28925 Alcorcón, Madrid, Spain

Correspondence

Prof. Gabriel Herrero-Beaumont,
Bone and Joint Research Unit
IIS-Fundación Jiménez Díaz-UAM
Rheumatology Department
Reyes Católicos, 2
28040 Madrid. Spain
+34 91550 49 78
GHerrero@fjd.es

Title character count: 96

Manuscript character count: 52396

ABSTRACT

Background: Chondrocytes in osteoarthritic (OA) cartilage acquire a hypertrophic-like phenotype, where Hedgehog (Hh) signaling is pivotal. Hh overexpression causes OA-like cartilage lesions, whereas its downregulation prevents articular destruction in mouse models. Mutations in *EVC* and *EVC2* genes disrupt Hh signaling, and are responsible for the Ellis-van Creveld syndrome skeletal dysplasia. Since Ellis-van Creveld syndrome protein (Evc) deletion is expected to hamper Hh target gene expression we hypothesized that it would also prevent OA progression avoiding chondrocyte hypertrophy. Our aim was to study Evc as a new therapeutic target in OA, and whether Evc deletion restrains chondrocyte hypertrophy and prevents joint damage in an Evc tamoxifen induced knockout (Evc^{cKO}) model of OA.

Methods: OA was induced by surgical knee destabilization in wild-type (WT) and Evc^{cKO} adult mice, and healthy WT mice were used as controls (n=10 knees/group). Hypertrophic markers and Hh genes were measured by qRT-PCR, and metalloproteinases (MMP) levels assessed by western blot. Human OA chondrocytes and cartilage samples were obtained from patients undergoing knee joint replacement surgery. Cyclopamine (CPA) was used for Hh pharmacological inhibition and IL-1β as an inflammatory insult.

Results: Tamoxifen induced inactivation of *Evc* inhibited Hh overexpression and partially prevented chondrocyte hypertrophy during OA, although it did not ameliorate cartilage damage in DMM-Evc^{cKO} mice. Hh pathway inhibition did not modify the expression of proinflammatory mediators induced by IL-1 beta in human OA chondrocytes in culture. Hypertrophic – IHH – and inflammatory – COX-2 – markers co-localized in OA cartilage samples.

Conclusions: Tamoxifen induced inactivation of *Evc* partially prevented chondrocyte hypertrophy in DMM-Evc^{cKO} mice, but it did not ameliorate cartilage damage. Our results suggest that chondrocyte hypertrophy per se is not a pathogenic event in the progression of OA.

Keywords: Osteoarthritis, Hedgehog, Chondrocyte Hypertrophy, Cartilage, Ellis-van Creveld.

INTRODUCTION

Osteoarthritis (OA) is a chronic joint disease mainly affecting articular cartilage, which undergoes erosion, characterized by extracellular matrix (ECM) degradation and cell alterations(1–5). Chronic biomechanical stress is the main factor triggering cartilage degradation(5). The resulting damage-associated molecular patterns (DAMPs) activate Toll-like receptors (TLR) and innate immunity in OA chondrocytes, evoking a local chronic inflammatory response with an increase in proinflammatory cytokines such as interleukin (IL)-1 or tumor necrosis factor (TNF). In turn, these cytokines induce the release of active metalloproteinases (MMP), aggrecanases and different proinflammatory mediators which activate the catabolic program characteristic of this disease(5). Together with inflammation, regenerative mechanisms are triggered by OA chondrocytes presumably as an attempt to repair the damagedtissue, such as the reactivation of signalling pathways operating during endochondral ossification of the growth plate, as Indian Hedgehog (IHH), WNT or NOTCH signaling(1,6,7). That is the reason why OA chondrocytes with this gene expression pattern are known as hypertrophic-like chondrocytes.

During limb development hypertrophic chondrocytes show a gradual increase in its cell size and varying gene expression, including Runt-related transcription factor 2 (RUNX2) and IHH, and progressively type X collagen (COL-10), MMP-13, receptor activator of nuclear factor kappa-B ligand (RANKL), and osteopontin (SPP1)(1,8). This developmental process, deeply coordinated by the IHH–parathyroid hormone-related protein (PTHrP) axis, drives an active ECM remodeling, until chondrocytes reach an apoptotic fate and leave a mineralized matrix for bone formation(1,8). Therefore, IHH has an essential role during embryonic and postnatal skeletal development and bone growth.

The Hedgehog (Hh) family of signaling molecules mediates the development of numerous organs during embryogenesis. However, In general, this signaling is physiologically repressed in the adult stage being only reactivated during tissue repair processes after injury, such as in lung epithelium, muscle, cartilage and bone(9).

Three Hh genes have been described in vertebrates, Sonic (SHH), Desert (DHH) and IHH, whose canonical signaling anchors to the primary cilium, a cellular structure highly specialized in the reception and transduction of mechanical and biochemical stimuli into the cell(10). Upon the arrival of a Hh ligand and its binding to the PTCH1 receptor, Smoothened (SMO) is released from PTCH1-mediated repression, and it translocates to the base of the cilium, where interacts with the EVC-EVC2 complex(11,12). This interaction promotes the activator function of the gliome associated oncogene (GLI)transcription factors and thus the expression of Hh

target genes, including Hh signaling components, such as PTCH1 and GLI1, and chondrocyte hypertrophy related genes(2,11–13).

Congruently with the hypertrophic-like phenotype, both human and animal OA cartilage exhibits increased levels of IHH and overexpression of components of the Hh pathway(14,15). Furthermore, chondrocytes in OA cartilage have also been described as morphologically hypertrophic cells with an increased size that are present in all the articular cartilage zones(16). These cell alterations also correlate with the expression of IHH in the cartilage and with the grade of tissue destruction(13,15,17). Experimental models have revealed that genetically modified mice with higher activation of Hh signaling (*Ptch1*$^{+/-}$, *Col2a1-Gli2*–transgenic and *COL2-rtTA-Cre;Gt(ROSA)26Sor*$^{tm1(Smo/YFP)Amc}$) show cartilage extracellular matrix remodeling, proteoglycan loss and chondrocyte fate alterations, together with an increased expression of chondrocyte hypertrophic markers, as *Col10a1* and *Mmp13*(14), although the characteristic cartilage OA lesions were not observed. On the contrary, Smo genetic downregulation (*COL2-rtTA-Cre;Smo*^{tm2Amc}) and conditional deletion (*Rosa-CreER(T);Smo*$^{fl/fl}$), and *Ihh* conditional deletion (*Col2a1-CreER*^{T2}*;Ihh*$^{fl/fl}$) attenuate surgically induced OA in mice(14,18,19). The effect of Hh pharmacological inhibition employing SMO and GLI inhibitors, such as cyclopamine (CPA) and GANT-61, has also been tested. The treatment with the Hh inhibitor $C_{31}H_{42}N_4O_5$prevents joint destruction in OA mice, and was associated with a decrease in OA markers, as *Adamts5* and *Col10a1*(14). The efficacy of these inhibitors on cartilage damage attenuation has also been tested in rodent models of severe OA, or adjuvant-induced arthritis(20,21).

On the other hand, blocking of SMO function results in a robust inhibition of Hh signaling(22,23). Potent SMO and GLI antagonists are particularly valuable for effectively inhibiting Hh signaling in several types of tumors with aberrant Hh activation, such as basal cell carcinoma and medulloblastoma(24). However, the accompanying adverse reactions, such as weight loss, fatigue, muscle spasms, alopecia, and dysgeusia(25), makes it questionable to consider SMO inhibitors as a feasible therapy for a chronic joint disease like OA.

Unlike other proteins of the Hh pathway, Evc works as a modulator of Hh signaling that lacks the critical role of other mediators of the Hh pathway, as SMO. In fact, a proportion of *Evc*$^{-/-}$ mice in a C57BL/6J;129 mixed background were found to be able to survive for at least 18 days after birth, albeit exhibiting severe skeletal defects(26), whereas *Smo*$^{-/-}$ mice do not survive beyond 9.5 days of embryonic development(27). This suggests that Evc silencing may result in a partial blockade of Hh signaling, and may represent a more plausible therapeutic target for Hh inhibition and downstream gene repression in OA cartilage.

Thus, we hypothesized that *Evc* deletion would prevent chondrocyte hypertrophy associated to OA. In order to test whether Evc should be considered as a new therapeutic target in OA, we used our previously reported *Evc* tamoxifen (TAM) induced conditional knockout (Evc^{cKO}) model(28) to specifically study if the blockade of Hh signaling and the entailing hypertrophy mechanisms exclusively during the adult stage could prevent the development of OA.

RESULTS

Evc levels are drastically diminished in $Evc^{flox/-}$ mice

Prior the study of *Evc* deletion on OA cartilage damage *in vivo*, we wanted to verify the efficacy of TAM on the deletion of *Evc* in adult Evc^{cKO} mice. We used RT-qPCR to study *Evc* transcript levels in mice treated with TAM (Evc^{cKO}) and with vehicle ($Evc^{flox/-}$) as well as in WT mice, which were used as the reference group for normal *Evc* gene expression levels in healthy status. As predicted, Evc^{cKO} mice did not express *Evc* in lung, heart, brain, muscle or bone tissue (Sup.Fig.1). Unexpectedly, *Evc* levels in $Evc^{flox/-}$mice were drastically decreased with respect to WT mice, being more similar to those observed in Evc^{cKO} animals (Sup.Fig.1). For this reason, WT mice, instead of $Evc^{flox/-}$, were selected as the control group to study the effect of *Evc* deletion on OA cartilage damage *in vivo*.

Evc deletion in DMM-Evc^{cKO} mice does not prevent OA-associated cartilage damage

We first studied cartilage damage in mice following 8 weeks post-surgery. Experimental OA due to knee joint destabilization evoked articular cartilage lesions in DMM-WT and DMM-Evc^{cKO} mice compared with their respective healthy controls(28). However, we found no amelioration in cartilage damage of DMM-Evc^{cKO} mice compared with DMM-WT animals, as showed by similar OARSI scores in both groups (Table 1).

Hh signaling is effectively blocked in DMM-Evc^{cKO} mice

Meniscal destabilization-induced OA was responsible for an induction in Hh related genes – *Ptch1*, *Gli1*, *Evc* and *Ihh* – in the knees of DMM-WT mice in comparison with NO-WT healthy individuals, while the expression of these genes was decreased in DMM-Evc^{cKO} mice compared with DMM-WT (Fig.1A-D). These results indicate that *Evc* deletion prevents Hh overexpression associated to OA.

Evc deletion does not prevent cartilage catabolism in DMM-Evc^{cKO} mice

We studied MMP protein profile in the mouse knees to further assess tissue damage in the joint and to determine if *Evc* deletion could attenuate cartilage catabolism in DMM-*Evc*^{cKO} mice. MMP-13, MMP-1 and MMP-3 protein levels increased in the knee joints of DMM-WT mice compared with NO-WT, while DMM-*Evc*^{cKO} mice showed similar MMP levels compared with DMM-WT animals (Fig.2A-F). This suggests that despite Hh blockade mediated by *Evc* inactivation, cartilage catabolism remains strongly active in DMM-*Evc*^{cKO} mice. The analysis of anabolic markers revealed substantial low levels of *Col2a1* gene expression in DMM-*Evc*^{cKO} mice, whereas *Agg* transcript levels were similar between groups (Fig.2G,H).

Chondrocyte hypertrophy is partially inhibited in DMM-*Evc*^{cKO} mice

The analysis of the gene expression levels of hypertrophic markers in the knee joints revealed increased levels of *Ihh*, *Col10a1* and *Alpl* during OA in DMM-WT mice, which decreased in the DMM-*Evc*^{cKO} group with respect to DMM-WT animals (Fig.1D, Fig.3B,E). *Runx2* and *Sp7* levels were also diminished in DMM-*Evc*^{cKO} mice compared with DMM-WT (Fig.3A,F). *Mmp13* and *Adamts5* mRNA levels were not modified between groups (Fig.3C,D).The thickness of the femur calcified cartilage showed an increasing trend in DMM-WT animals with respect to NO-WT mice, and decreased in DMM-*Evc*^{cKO} mice compared with the DMM-WT group (Fig.3G,H). These results suggest a relevant role of Evc in the hypertrophy and calcification process associated to OA in this model.

Human OA cartilage co-expresses hypertrophic and inflammatory phenotypes

We suspected that the blockade of the hypertrophy response could trigger a higher inflammatory activation in OA chondrocytes. This would explain the fact that despite blocking hypertrophy we did not see improvement in cartilage damage in DMM-*Evc*^{cKO} mice. To test this premise, we first aimed to determine whether chondrocytes polarize towards the acquisition of a hypertrophic vs an inflammatory phenotype in OA cartilage. With this purpose we analyzed the presence of IHH and COX-2 in human cartilage samples by immunofluorescence (Fig.4A,B). We found that both proteins co-localized in the same cells and areas in human OA cartilage (Fig.4D), suggesting that chondrocytes can express both hypertrophic and inflammatory proteins at the same time. This result demonstrates the coexistence of both pathological phenotypes in the same cell.

Human OA chondrocytes inflammatory response is not modified by Hh inhibition

Once we observed that both hypertrophic and inflammatory phenotypes co-localize in the same cell, we aimed to determine whether both signaling processes interact and mutually

regulate in OA chondrocytes. We studied if IL-1 beta-mediated inflammatory response could indirectly modify the synthesis of hypertrophic differentiation inducers in human OA chondrocytes. IL-1 beta insult decreased *GLI1* and *EVC* gene expression levels in IL-1 beta-stimulated chondrocytes compared with control cells (Fig.5B,C), and increased *IHH* gene expression levels (Fig.5D), while no changes were observed in *PTCH1* expression (Fig.5A). Then, we deepened in the inflammatory study in human OA chondrocytes to determine the effect of Hh signaling blockade on the response of chondrocytes to IL-1 beta-induced inflammation. We used CPA as a Hh inhibitor due to its direct antagonism by interaction with SMO(29). CPA-mediated Hh inhibition did not modify the gene expression of pro-inflammatory markers – *IL1B*, *MMP13*, *PTGS2*, *PTGER2*, *IL6*, *NOS2* and *CCL2* – with respect to chondrocytes not treated with the SMO inhibitor (Fig.5E-K). These data indicate that Hh inhibition, and therefore hypertrophy blockade, does not alter OA chondrocytes inflammatory response to IL-1 beta.

DISCUSSION

Our results show that surgically-induced OA in mice induced the activation of the Hh pathway, increasing *Ptch1*, *Gli1* and *Ihh* gene expression in the OA knees, as previous studies have observed in rodent models of OA(14,30). In addition, we observed that *Evc* levels were also increased in OA mouse knee joints.

The role of EVC and its specific activation have not been previously described in OA. Since EVC positively mediates Hh signaling, and DMM induces its overexpression, we proposed EVC as a new therapeutic target for inhibiting chondrocyte hypertrophy-like phenomena that are activated in OA. In addition, the expression of *Evc* seems to be mainly limited to cartilage tissue(26,31). Thus, a selective EVC inhibition would be specifically directed to articular hyaline cartilage in comparison to different Hh inhibitors that have a widespread effect in different tissues and organs.

Hh signaling has an essential role in limb and neural development and is dysregulated in disease states, such as in genetic (e.g. Bardet–Biedl syndrome) or neurodegenerative disorders (e.g. Parkinson's and Alzheimer's disease), cancer (e.g. basal cell carcinoma (BCC) and medulloblastoma), and OA(32,33). Hh function is also required for tissue repair and homeostasis, in coordination with WNT and TGF-beta/BMP signaling and G protein-coupled receptors actions(33), for example in lung epithelium regeneration(34), epidermal and hair follicle maintenance(35), and muscle regeneration(9).

The mechanisms of Hh signaling inhibition at different levels of the pathway have been deeply studied in the context of cancer research. Different Hh pharmacological inhibitors are

238 available for cancer treatment, mainly SMO and GLI1 inhibitors, which effectively suppress Hh
239 activation(36,37). These Hh-targeted drugs have shown their efficacy in the treatment of a
240 variety of tumors, including BCC, pancreatic or breast cancer(37). However, these Hh inhibitors,
241 like vismodegib and sonidegib, are associated with different adverse events such as muscle
242 spasms, alopecia, dysgeusia, weight loss, and fatigue(25,38).

243 The experimental use of these inhibitors in OA models has proven that SMO and GLI
244 pharmacological inhibitors strongly restrain Hh signaling and exert a protective effect against
245 OA progression(14,39,40). OA mice treated with the SMO inhibitor $C_{31}H_{42}N_4O_5$ showed
246 articular cartilage recovery, as well as a downregulation of *Ptch1, Gli1*, and Hh interacting
247 protein (*Hhip*), together with a decrease in the hypertrophic markers *Adamts5* and
248 *Col10a1*(14). In rats with adjuvant-induced arthritis, CPA reduced cartilage damage and
249 inflammation, diminishing TNF-a, IL-1 beta, and IL-6 serum levels(21). Furthermore, the GLI
250 inhibitor GANT-61, in combination with a low dose of the anti-inflammatory indomethacin,
251 was found to synergistically reduce cartilage damage and inflammatory cytokines TNF-a, IL-2,
252 and IL-6 in serum, through pyroptosis inhibition in chondrocytes(20).

253 Although these Hh inhibitory molecules have been tested in experimental OA models and
254 have given promising results, the use of these compounds for the treatment of human OA does
255 not seem acceptable due to their toxicity and the above mentioned associated adverse effects.
256 Also, their long-term effects on the arthritic joint itself, and in other regenerative processes
257 such as bone fracture healing, are still undefined. Due to the less critical nature of Evc in
258 comparison to other mediators of the Hh pathway, Evc inhibition would provide a more
259 plausible target for the treatment of OA. Although half of *Evc* knockouts were reported to die
260 soon after birth, some can survive to adulthood under special heed in a C57BL/6J;129 mixed
261 genetic background. In contrast, *Smo* knockouts fail embryonic development and die at
262 E9.5(26,32,41). Thus, Evc blockade would display a partial inhibition of the Hh pathway in
263 comparison with the vast inhibition induced by the blockade of other mediators, such as SMO
264 or IHH.

265 Aside from the classical Hh activation, several pathways such as MAPK/MEK/ERK,
266 PI3K/AKT/mTOR, TGF-beta and PKC signaling, modulate GLI1 and GLI2 transcriptional activity
267 through non-canonical Hh activation(42). Particularly in OA, Hh signaling interacts with the
268 NOTCH, WNT, FGF and mTOR pathways(2). Furthermore, inflammatory pathways such as TNF-
269 a/mTOR, potentiate GLI1 activity in a SMO-independent manner(43,44).Overall, signaling
270 cascades and cellular responses triggered by Hh pathway seem to be highly context-
271 dependent(2).

We utilized an *Evc*^{cKO} model in mice females combined with DMM, and we demonstrated that *Evc*^{cKO} effectively inhibited Hh signaling overexpression during OA triggered by DMM, and decreased chondrocyte hypertrophic markers. We employed this OA model, in which mice developed mild to moderate OA alterations(45), in order to test plausible beneficial effects of hypertrophy blockade. We observed a general decrease in the expression of *Ihh*, *Runx2*, *Col10a1*, *Alpl* and *Sp7* in the joints of DMM-*Evc*^{cKO} mice in comparison to DMM-WT animals. Furthermore, tamoxifen induced inactivation of Evc accounted for a substantial prevention of calcified cartilage thickening in DMM-*Evc*^{cKO} mice compared to DMM-WT mice.

Although *Evc*^{cKO} showed a decrease in Hh induction induced by OA, together with a lower hypertrophy and calcification progression, no amelioration of cartilage damage was observed in DMM-*Evc*^{cKO} mice compared with DMM-WT. We have previously demonstrated that DMM-WT and DMM-*Evc*^{cKO} mouse joints also exhibited similar subchondral bone sclerosis associated to DMM(28).

Research in *Evc* null mice have shed light on its physiological role and demonstrated that EVC localises at the base of the primary cilium and mediates Hh signaling in chondrocytes and osteoblasts(26,46). Still, the role of Evc in the cartilage seems to be restricted to skeletal development and bone growth, with an unclear role in the adult tissue. Specifically in OA, studies have been conducted investigating the function of the primary cilium in chondrocytes. An increased cilium lengthand prevalence of ciliated chondrocytes have been associated to tissue erosion and mild to severe OA lesions in the cartilage(47,48). Also cilia orientation undergoes alterations in the OA cartilage. While healthy chondrocytes orient their cilium away from the cell surface, chondrocytes in OA cartilage direct their primary cilia into the core of OA chondrons(48). Alterations in primary cilium structure and assembly have also been associated with a Hh-mediated mechanosensitive diminished response in bovine articular chondrocytes(49). Similarly, primary cilium depletion in chondrocytes is responsible for impeded GLI3 processing to the repressor form of the transcription factor, thus promoting increased Hh signaling and OA markers(50). *Evc*$^{-/-}$ chondrocytes do not show alterations in ciliogenesis(26). Yet, *Evc* absence does produce chondrocyte dysfunction, as can be asserted by the severe skeletal and growth alterations of *Evc*$^{-/-}$and growth plate column disarrangement in *Evc*^{cKO} adult mice(26,28). It still remains unknown how inactivation of Evc in *Evc*^{cKO} mice might influence articular cartilage quality in the long term.

The extremely low *Col2a1* transcript levels found in DMM-*Evc*^{cKO} mice are consistent with the alteration of the genetic locus of *COL2A1* in patients with osteochondrodysplasias(51). In an Ellis–van Creveld experimental model in calf with an *EVC2* mutation, abnormal COL2A1 expression was histologically found in the physis, attributed to an accelerated COL2A1

307 degradation(52). In contrast, our data show a COL2A1 synthesis defect in DMM-*Evc*^{cKO} mice.
308 The low *Col2a1* transcript levels, together with the relatively high MMP-associated catabolism,
309 particularly MMP-13 and MMP-1, maintained in the knee joints of DMM-*Evc*^{cKO} mice, may have
310 contributed to a more rapid progression of cartilage damage in DMM-*Evc*^{cKO} mice than a priori
311 anticipated. Both findings matched histological cartilage damage in DMM-*Evc*^{cKO} joints and its
312 equal OA progression to DMM-WT mice(28).

313 Both hypertrophy-like alterations and inflammation in OA chondrocytes have been
314 described as characteristic phenomena in this disease. Recent data from our laboratory
315 demonstrate that hypertrophic chondrocytes can be found in all hyaline cartilage layers, and
316 not within a specific location(16). In this work, we have demonstrated that these signals can be
317 simultaneously found in OA chondrocytes, since we were able to co-localize IHH and COX-2 in
318 human OA chondrocytes. The co-localization of both hypertrophy and inflammatory markers in
319 human OA cartilage suggests that the acquisition of the hypertrophic-like phenotype does not
320 exclude the expression of an inflammatory profile. Our data indicate the presence of a
321 complex signaling network modulating chondrocyte responses in OA.

322 In line with this data, it could be possible that IHH-signaling down-regulation observed in
323 *Evc*^{cKO} mice could exacerbate the inflammatory response in OA chondrocytes, being
324 responsible for the absence of a protective effect on cartilage degradation observed in DMM-
325 *Evc*^{cKO} mice, in comparison to DMM-WT. In fact, it has been previously shown that both
326 pathways could be able to regulate each other. IL-1 beta stimulation would decrease the
327 activation of the Hh pathway(53), while Hh activation has been long associated with OA
328 cartilage degradation due to an increase in catabolic enzymes such as ADAMTS5 and MMP-
329 13(13,14,18). However, Thompson and co-workers observed that Hh pathway activation
330 induced by recombinant-Ihh did not stimulate cartilage degradation in healthy bovine articular
331 chondrocytes(53). On the other hand, some reports have even postulated that Hh may induce
332 anti-inflammatory responses(54,55). Genetic or pharmacologic Hh inhibition increased the
333 presence of inflammatory mediators, whereas *Gli1* overexpression seemed to ameliorate
334 inflammatory outcomes in mouse models of colitis and acute pancreatitis through the
335 induction of the anti-inflammatory cytokine IL-10(54,55).

336 Thus, employing *in vitro* studies, we investigated whether Hh signaling inhibition might
337 trigger a higher inflammatory response in human OA chondrocytes. Our data indicated that IL-
338 1 beta accounted for an inhibition in Hh pathway in human OA chondrocytes, particularly
339 decreasing *GLI1* and *EVC* gene expression. In contrast, we observed that human OA
340 chondrocytes did not modify their inflammatory response to IL-1 beta under Hh pathway
341 inhibition.

342 Overall, our results showed that *Evc*-mediated Hh inactivation partially prevented
343 chondrocyte hypertrophy but did not ameliorate OA cartilage damage in DMM-*Evc*^{cKO} mice.
344 These data suggest that a partial blockade of the Hh pathway through tamoxifen induced
345 inactivation of *Evc* is not a therapeutic target for mild/incipient OA. In this OA model, we have
346 demonstrated that chondrocyte hypertrophy was associated to Hh signaling activation, but it is
347 not a pathogenic event in the development of the disease. In this sense, chondrocyte
348 hypertrophy could be a frustrated regenerative mechanism that correlates with OA
349 progression, but not a leading cause of cartilage degeneration per se.
350

351 **MATERIALS AND METHODS**

Reagents and Tools	
Material	**Supplier**
Rabbit polyclonal anti-mouse MMP-13 (1/6000; ab39012)	Abcam, Cambridge, UK
Rabbit polyclonal anti-mouse MMP-1 (1/500; ab137332)	Abcam, Cambridge, UK
Rabbit monoclonal anti-mouse MMP-3 (1/10000; ab52915)	Abcam, Cambridge, UK
EZ-Blue gel staining reagent	Sigma-Aldrich, St Louis, MO, USA
TRIzol reagent	MRC, Cincinnati, OH, USA
TaqMan probes: *Ptch1* (Mm00436026_m1), *Evc* (Mm00469587_m1), *Gli1* (Mm00494645_m1), *Ihh* (Mm00439613_m1), *Runx2* (Mm00501584_m1), *Col10a1* (Mm00487041_m1), *Mmp13* (Mm00439491_m1), *Adamts5* (Mm00478620_m1), *Alpl* (Mm00475834_m1), *Sp7* (Mm00504574_m1), *Col2a1* (Mm01309565_m1), *Agg* (Mm00545794_m1), *Hprt1* (Mm00446968_m1), *PTCH1* (Hs00181117_m1), *EVC* (Hs00205772_m1), *GLI1* (Hs00171790_m1), *IHH* (Hs01081801_m1), *IL1B* (Hs00174097_m1), *MMP13 (), PTGS2* (Hs00610420_m1), *PTGER2* (Hs00168754_m1), *IL6* (Hs00174131_m1), *NOS2* (Hs00167257_m1), *CCL2 (), HPRT1* (Hs99999909_m1)	Applied Biosystems, CA, USA
Dulbecco's Modified Eagle Medium (DMEM) 1 g/L glucose	Lonza, Basel, Switzerland
Fetal bovine serum (FBS)	Sigma-Aldrich, St Louis, MO, USA
L-Glutamine	Lonza, Basel, Switzerland
Penicillin-Streptomycin	Lonza, Basel, Switzerland
IL-1 beta	Peprotech, London, UK

Cyclopamine (CPA) (C4116)	Sigma-Aldrich, St Louis, MO, USA
Proteinase K	Promega, Madison, WI, USA
Triton X-100	Sigma-Aldrich, St Louis, MO, USA
Rabbit polyclonal anti-IHH (1/100; ab39634)	Abcam, Cambridge, UK
Mouse polyclonal anti- COX-2 (1/100; ab88522).	Abcam, Cambridge, UK
Fluoroshield with DAPI histology mounting medium	Sigma-Aldrich, St Louis, MO, USA
iScanCoreo Au version 3.3.3	Roche, Basel, Switzerland
Image Viewer software	Ventana Medical Systems, USA
Amersham Imager 600	Healthcare, Little Chalfont, Buckinghamshire, UK
Step One Plus Detection system	Applied Biosystems, CA, USA
G-power 3.1 software	G-power, Autenzell, Germany
GraphPad Prism 8 for Windows	GraphPad Software, San Diego, CA, USA

Methods and Protocols

Animal model of OA

Generation of *Evc*$^{flox/-}$; UBC-*CreERT2* mice was previously described(28). These mice were maintained in a C57BL/6J;129 mixed background. Briefly, 10 weeks-old *Evc*$^{flox/-}$;*UBC-CreERT2*$^{+/-}$ female mice received vehicle or 0.075 mg/g/day TAM administered in five intraperitoneal injections. Vehicle-treated mice were named as *Evc*$^{flox/-}$ and TAM-treated mice as *Evc*^{cKO}. C57BL/6J;129 WT mice were used as controls due to unexpected low *Evc* levels in *Evc*$^{flox/-}$mice (Sup.Fig.1). Mice were separated and housed in cages according to their genotype to avoid tamoxifen contamination, were exposed to 12-hour light/dark cycles, and had free access to water and standard chow. OA was induced at 12 weeks of age by destabilization of the medial meniscus (DMM) as previously described(28,45), and mice were assigned to groups of study according to their genotype and randomly distributed between healthy and DMM-operated: non-operated (NO)-WT (n=8), DMM-WT (n=6)and DMM-*Evc*^{cKO} (n=6). After 8 weeks of OA progression, mice were euthanized and tissues and joints collected for histopathological and molecular analysis. Tissue samples from brain, lung, muscle, heart, bone and joints were immediately frozen for molecular biology studies. Animal handling and experimental procedures for this study (PROEX 119/16) complied with the national and international regulations, and the Guidelines for the Care and Use of Laboratory Animals (NIH), and were

371 approved by the Institutional Ethics and Welfare Committees of the IIS-Fundación Jiménez Díaz
372 and Alberto Sols Biomedical Research Institute.
373
374 **Cartilage thickness analyses**
375 Cartilage thickness was evaluated in knee sections stained with Hematoxylin/Eosin and
376 scanned with the iScanCoreo Au version 3.3.3 (Roche, Basel, Switzerland). A 500 µm line was
377 drawn covering the center and posterior region of the joint in the femur using the Image
378 Viewer software (Ventana Medical Systems, USA), and calcified cartilage area was calculated
379 using the Image J software.
380
381 **Western blotting**
382 20 µg of protein extract from knee joints were separated by SDS-PAGE and transferred to
383 nitrocellulose membranes as previously described(56,57). Membranes were incubated
384 overnight at 4°C with the following antibodies: rabbit polyclonal anti-mouse MMP-13 (1/6000;
385 ab39012; Abcam) and MMP-1 (1/500; ab137332; Abcam), and rabbit monoclonal anti-mouse
386 MMP-3 (1/10000; ab52915; Abcam). Binding signal was detected with chemiluminescence in
387 an Amersham Imager 600 (Healthcare, Little Chalfont, Buckinghamshire, UK). EZ-Blue gel
388 staining reagent (Sigma) was used as loading control and densitometric measures were
389 normalized by the average value of the NO-WT and expressed as arbitrary units (A.U.)(56–58).
390
391 **RNA isolation and gene expression assays**
392 RNA was isolated from frozen knees, prior crush in liquid nitrogen, by TRIzol reagent
393 (MRC, Cincinnati, OH, USA) and retrotranscribed to cDNA as described elsewhere(56). RNA
394 from chondrocyte cultures was also isolated with TRIzol reagent. Gene expression was
395 quantified by real-time PCR using the Step One Plus Detection system (Applied Biosystems, CA,
396 USA). TaqMan probes for mouse *Ptch1*, *Evc*, *Gli1*, *Ihh*, *Runx2*, *Col10a1*, *Mmp13*, A disintegrin
397 and metalloproteinase with thrombospondin motifs 5 (*Adamts5)*, Alkaline phosphatase (*Alpl)*,
398 Transcription factor SP7 (*Sp7)*, type II collagen (*Col2a1*) and aggrecan (*Agg*), and TaqMan
399 probes for human *PTCH1*, *EVC*, *GLI1*, *IHH, IL1B*, *MMP13*, prostaglandin G/H synthase 2 (*PTGS2*),
400 prostaglandin E2 receptor (*PTGER2*), *IL6*, inducible nitric oxide synthase (*NOS2*) and monocyte
401 chemoattractant protein-1 (*CCL2*) were purchased from Applied Biosystems. Gene expression
402 levels were determined with the comparative Ct quantitation method using Hypoxanthine-
403 guanine phosphoribosyltransferase (*Hprt1, HPRT1)* as internal control and expressed as
404 arbitrary units (A.U.).
405

406 **Human OA cartilage collection for chondrocyte isolation**

407 Human OA cartilage was obtained from patients undergoing knee joint replacement
408 surgery (Fundación Jiménez Díaz Hospital), prior informed consent and approval from the
409 Institutional Ethics Committee, and following the ethical principles of the Declaration of
410 Helsinki and the Department of Health and Human Services Belmont Report. Chondrocytes
411 were isolated as previously described(59).

412

413 **Culture of human chondrocytes**

414 Human OA chondrocytes were seeded at a confluence of $2 \cdot 10^5$ cells/well in p6 plates with
415 Dulbecco's Modified Eagle Medium (DMEM) 1 g/L glucose, supplemented with 10% fetal
416 bovine serum (FBS)(Sigma), 2 mM glutamine (Lonza), and 100 U/ml Penicillin-Streptomycin
417 (PS) (Lonza). Experiments were performed in passage 2. Cells were FBS-depleted for 24 hours,
418 and then stimulated with 1 ng/mL IL-1 beta (Peprotech, London, UK), and 10 µM CPA (Sigma),
419 a direct Hh antagonist(29), for 24 hours. Chondrocytes not stimulated with IL-1 beta nor CPA
420 were used as control. Each experiment was performed with chondrocytes from different
421 donors.

422

423 **Immunofluorescence of human cartilage**

424 Immunofluorescence was performed based on previously described protocols(60). Briefly,
425 3 µm knee joint sections were deparafinized and rehydrated. Antigen retrieval was performed
426 by incubation with 20 µg/mL proteinase K (Promega, USA) for 20 minutes. Tissue sections were
427 incubated with 0.1 M glycine for autofluorescence removal, and blocked with 3% PBS-bovine
428 serum albumin (BSA), 0.1% Triton X-100 (Sigma), 5% FBS. Then cartilage sections were
429 incubated with the corresponding primary antibodies: rabbit polyclonal anti-IHH (1/100;
430 ab39634, Abcam) and mouse polyclonal anti-Cyclooxygenase-2 (COX-2) (1/100; ab88522;
431 Abcam). Secondary FITC and TRITC respectively antibodies were used for detection of positive
432 fluorescence signal. Tissue sections were ultimately incubated with 0.1% Sudan Black in 70%
433 ethanol and mounted with Fluoroshield with DAPI histology mounting medium (Sigma).
434 Sections were photographed with a MiCom fluorescence microscope equipped with ACT-1
435 software at ×40 magnification.

436

437 **Statistical analysis**

438 An animal model previously studied(28)was used for the attainment of the present
439 research. Each limb was analyzed as an independent sample. Due to the lack of previous
440 studies of OA in mice with *Evc* deletion, previously published data of an OA model with *Ihh*

deletion was used for the calculation of the sample size(18). The sample size was determined with the objective of detecting differences with respect to the articular cartilage damage score between OA and OA *Col2a1-CreERT2; Ihh*$^{fl/fl}$ mice. By accepting a significance level (alpha) of 5% assuming a Bonferroni correction, and a statistical power of 80%, a pairwise t-test between conditions required 6 limbs per group to demonstrate an 86% (7 vs 1 damage score with the *OARSI Osteoarthritis Cartilage Histopathology Assessment System* (OOCHAS) scale assuming a standard deviation of 3 and 2 respectively. Sample size estimation was performed using the G-power 3.1 software (G-power, Autenzell, Germany)(61), which indicated no requirement of additional animals to the study in order to detect the expected differences in cartilage damage between groups.

Ordinary one-way ANOVA with Bonferroni post-hoc test was used for comparisons between groups with normal distribution of the data, based on Shapiro-Wilk normality test. Kruskal-Wallis test was used for comparisons between multiple groups where data lacked normality, followed by Dunn's post-hoc test. A P-value of less than 0.05 was considered statistically significant. Statistical analyses of data were performed using GraphPad Prism 8 for Windows (GraphPad Software, San Diego, CA, USA). Data were expressed as mean with standard error (SEM).

Acknowledgements

This work was financially supported by grants from the Instituto de Salud Carlos III [PI15/00340, PI16/00065, PI18/00261] and Fondo Europeo de Desarrollo Regional (FEDER) and by grants SAF-2013-43365-R and SAF2016-75434-R to VLR-P. AL and PG were funded by Fundación Conchita Rábago. We would like to thank Dr. David Santamaria for providing UBC-*CreERT2* mice and María Gracia González Bueno for helping to organize mouse crosses and technical work.

Author contributions

AL, VLR-P, RL and GH-B were in charge of conceptualization, formal analysis, and interpretation of data. VLR-P, GH-B and RL were responsible for the funding acquisition, provision of resources and project administration. AL, PG, LC, VLR-P, AP-C and RL were in charge of in charge of animal methodology design. LC, VLR-P and AP-C generated the genetically modified *Evc*^{cKO} model, and AL, PG, SP-N and RL performed the animal procedures. AL and PG contributed to the acquisition of data, investigation and visualization. AL, PG, LC, VLR-P, AP-C, SP-N, AM, GH-B and RL were involved in the writing process and drafting the article and its revision and editing, and approved the final manuscript to be published. GH-B and RL have full

476 access to overall data and take responsibility for the supervision, validation, integrity and
477 accuracy of the data analysis.

478

479 **Conflict of interest**

480 AL, PG, LC, VLR-P, AP-C, SP-N, AM, GH-B and RL do not have any disclosures.

481

482 **REFERENCES**

483 1. Singh P, Marcu KB, Goldring MB, Otero M. Phenotypic instability of chondrocytes in
484 osteoarthritis: on a path to hypertrophy. Annals of the New York Academy of Sciences.
485 2018;1442(1):17-34.

486 2. Ripmeester EG, Timur UT, Caron MM, Welting TJ. Recent Insights into the Contribution of
487 the Changing Hypertrophic Chondrocyte Phenotype in the Development and Progression
488 of Osteoarthritis. Frontiers in Bioengineering and Biotechnology. 2018;6(18):1-25.

489 3. Martel-Pelletier J, Barr AJ, Cicuttini FM, Conaghan PG, Cooper C, Goldring MB, et al.
490 Osteoarthritis. Nature Reviews Disease Primers. 2016;2(16072).

491 4. Loeser RF, Goldring SR, Scanzello CR, Goldring MB. Osteoarthritis: A disease of the joint
492 as an organ. Arthritis and Rheumatism. 2012;64(6):1697-707.

493 5. Herrero-Beaumont G, Pérez-Baos S, Sánchez-Pernaute O, Roman-Blas JA, Lamuedra A,
494 Largo R. Targeting chronic innate inflammatory pathways, the main road to prevention of
495 osteoarthritis progression. Biochemical Pharmacology. 2019;165:24-32.

496 6. Dunaeva M, Waltenberger J. Hh signaling in regeneration of the ischemic heart. Cellular
497 and Molecular Life Sciences. 2017;74(19):3481-90.

498 7. Giarretta I, Gaetani E, Bigossi M, Tondi P, Asahara T, Pola R. The Hedgehog Signaling
499 Pathway in Ischemic Tissues. International journal of molecular sciences. 2019;20(21):1-
500 19.

501 8. Kozhemyakina E, Lassar AB, Zelzer E. A pathway to bone: signaling molecules and
502 transcription factors involved in chondrocyte development and maturation.
503 Development. 2015;142(5):817-31.

504 9. Petrova R, Joyner AL. Roles for Hedgehog signaling in adult organ homeostasis and
505 repair. Development (Cambridge, England). 2014;141(18):3445-57.

506 10. Ruhlen R, Marberry K. The chondrocyte primary cilium. Osteoarthritis and Cartilage.
507 2014;22(8):1071-6.

508 11. Briscoe J, Thérond PP. The mechanisms of Hedgehog signalling and its roles in
509 development and disease. Nature Reviews Molecular Cell Biology. 2013;14(7):416-29.

510 12. Caparros-Martin JA, Valencia M, Reytor E, Pacheco M, Fernandez M, Perez-Aytes A, et al.
511 The ciliary Evc / Evc2 complex interacts with Smo and controls Hedgehog pathway
512 activity in chondrocytes by regulating Sufu / Gli3 dissociation and Gli3 trafficking in
513 primary cilia. Human Molecular Genetics. 2013;22(1):124-39.

514 13. Zhou J, Wei X, Wei L. Indian Hedgehog, a critical modulator in osteoarthritis, could be a
515 potential therapeutic target for attenuating cartilage degeneration disease. Connective
516 Tissue Research. 2014;55(4):257-61.

517 14. Lin AC, Seeto BL, Bartoszko JM, Khoury MA, Whetstone H, Ho L, et al. Modulating
518 hedgehog signaling can attenuate the severity of osteoarthritis. Nature Medicine.
519 2009;15(12):1421-5.

520 15. Zhang C, Wei X, Chen C, Cao K, Li Y, Jiao Q. Indian Hedgehog in Synovial Fluid Is a Novel
521 Marker for Early Cartilage Lesions in Human Knee Joint. 2014;7250-65.

522 16. Gratal P, Mediero A, Sánchez-Pernaute O, Prieto-Potin I, Lamuedra A, Herrero-Beaumont
523 G, et al. Chondrocyte enlargement is a marker of osteoarthritis severity. Osteoarthritis
524 and Cartilage. 2019;27(8).

525 17. Wei F, Zhou J, Wei X, Zhang J, Fleming BC, Terek R, et al. Activation of Indian hedgehog
526 promotes chondrocyte hypertrophy and upregulation of MMP-13 in human
527 osteoarthritic cartilage. Osteoarthritis and Cartilage. 2012;20(7):755-63.

528 18. Zhou J, Chen Q, Lanske B, Fleming BC, Terek R, Wei X, et al. Disrupting the Indian
529 hedgehog signaling pathway in vivo attenuates surgically induced osteoarthritis
530 progression in Col2a1-CreERT2; Ihhfl/fl mice. Arthritis Research and Therapy.
531 2014;16(1):R11.

532 19. Takada S, Nakamura E, Sabanai K, Tsukamoto M, Otomo H, Kanoh S, et al. Attenuation of
533 Post-Traumatic Osteoarthritis After Anterior Cruciate Ligament Injury Via Inhibition of
534 Hedgehog Signaling. Journal of Orthopaedic Research. 2019;

535 20. Liu Q, Wu Z, Hu D, Zhang L, Wang L, Liu G. Low dose of indomethacin and Hedgehog
536 signaling inhibitor administration synergistically attenuates cartilage damage in
537 osteoarthritis by controlling chondrocytes pyroptosis. Gene. 2019;712(143959).

538 21. Li R, Cai L, Ding J, Hu CM, Wu TN, Hu XY. Inhibition of hedgehog signal pathway by
539 cyclopamine attenuates inflammation and articular cartilage damage in rats with
540 adjuvant-induced arthritis. Journal of Pharmacy and Pharmacology. 2015;67(7):963-71.

541 22. Shen F, Cheng L, Douglas AE, Riobo NA, Manning DR. Smoothened is a fully competent
542 activator of the heterotrimeric G protein G(i). Mol Pharmacol. marzo de 2013;83(3):691-
543 7.

544 23. Peluso MO, Campbell VT, Harari JA, Tibbitts TT, Proctor JL, Whitebread N, et al. Impact of
545 the Smoothened inhibitor, IPI-926, on smoothened ciliary localization and Hedgehog
546 pathway activity. PLoS One. 2014;9(3):e90534.

547 24. Rimkus TK, Carpenter RL, Qasem S, Chan M, Lo H-W. Targeting the Sonic Hedgehog
548 Signaling Pathway: Review of Smoothened and GLI Inhibitors. Cancers (Basel). 15 de
549 febrero de 2016;8(2):E22.

550 25. Gutzmer R, Solomon JA. Hedgehog Pathway Inhibition for the Treatment of Basal Cell
551 Carcinoma. Target Oncol. junio de 2019;14(3):253-67.

552 26. Ruiz-Perez VL, Blair HJ, Rodriguez-Andres ME, Blanco MJ, Wilson A, Liu Y-N, et al. Evc is a
553 positive mediator of Ihh-regulated bone growth that localises at the base of chondrocyte
554 cilia. Development. 2007;134(16):2903-12.

555 27. Zhang XM, Ramalho-Santos M, McMahon AP. Smoothened mutants reveal redundant
556 roles for Shh and Ihh signaling including regulation of L/R asymmetry by the mouse node.
557 Cell. 2001;106(2):781-92.

558 28. Lamuedra A, Gratal P, Calatrava L, Ruiz-Perez VL, Largo R, Herrero-Beaumont G.
559 Disorganization of chondrocyte columns in the growth plate does not aggravate
560 experimental osteoarthritis in mice. Scientific Reports. 2020;10(1):1-13.

561 29. Bruce SJ, Butterfield NC, Metzis V, Town L, McGlinn E, Wicking C. Inactivation of
562 patched1 in the mouse limb has novel inhibitory effects on the chondrogenic program.
563 Journal of Biological Chemistry. 2010;285(36):27967-81.

564 30. Xu T, Xu G, Gu Z, Wu H. Hedgehog signal expression in articular cartilage of rat
565 temporomandibular joint and association with adjuvant-induced osteoarthritis. J Oral
566 Pathol Med. abril de 2017;46(4):284-91.

567 31. Will AJ, Cova G, Osterwalder M, Chan WL, Wittler L, Brieske N, et al. Composition and
568 dosage of a multipartite enhancer cluster control developmental expression of Ihh
569 (Indian hedgehog). Nature Genetics. 2017;49(10):1539-45.

570 32. Sasai N, Toriyama M, Kondo T. Hedgehog Signal and Genetic Disorders. Front Genet. 8 de
571 noviembre de 2019;10:1103.

572 33. Anvarian Z, Mykytyn K, Mukhopadhyay S, Pedersen LB, Christensen ST. Cellular signalling
573 by primary cilia in development, organ function and disease. Nat Rev Nephrol. abril de
574 2019;15(4):199-219.

575 34. Wang C, Cassandras M, Peng T. The Role of Hedgehog Signaling in Adult Lung
576 Regeneration and Maintenance. J Dev Biol. 9 de julio de 2019;7(3):E14.

577 35. Abe Y, Tanaka N. Roles of the Hedgehog Signaling Pathway in Epidermal and Hair Follicle
578 Development, Homeostasis, and Cancer. J Dev Biol. 20 de noviembre de 2017;5(4):E12.

579 36. Peer E, Tesanovic S, Aberger F. Next-Generation Hedgehog/GLI Pathway Inhibitors for
580 Cancer Therapy. Cancers (Basel). 15 de abril de 2019;11(4):E538.

581 37. Cortes JE, Gutzmer R, Kieran MW, Solomon JA. Hedgehog signaling inhibitors in solid and
582 hematological cancers. Cancer Treat Rev. junio de 2019;76:41-50.

583 38. Lacouture ME, Dréno B, Ascierto PA, Dummer R, Basset-Seguin N, Fife K, et al.
584 Characterization and Management of Hedgehog Pathway Inhibitor-Related Adverse
585 Events in Patients With Advanced Basal Cell Carcinoma. Oncologist. octubre de
586 2016;21(10):1218-29.

587 39. Rohatgi R, Milenkovic L, Corcoran RB, Scott MP. Hedgehog signal transduction by
588 Smoothened: Pharmacologic evidence for a 2-step activation process. Proceedings of the
589 National Academy of Sciences of the United States of America. 2009;106(9):3196-201.

590 40. Chen JK, Taipale J, Cooper MK, Beachy PA. Inhibition of Hedgehog signaling by direct
591 binding of cyclopamine to Smoothened. Genes and Development. 2002;16(21):2743-8.

592 41. Zhang XM, Ramalho-Santos M, McMahon AP. Smoothened mutants reveal redundant
593 roles for Shh and Ihh signaling including regulation of L/R asymmetry by the mouse node.
594 Cell. 2001;106(2):781-92.

595 42. Pietrobono S, Gagliardi S, Stecca B. Non-canonical Hedgehog Signaling Pathway in
596 Cancer: Activation of GLI Transcription Factors Beyond Smoothened. Front Genet.
597 2019;10:556.

598 43. Didiasova M, Schaefer L, Wygrecka M. Targeting GLI Transcription Factors in Cancer.
599 Molecules. 24 de abril de 2018;23(5):E1003.

600 44. Wang Y, Ding Q, Yen C-J, Xia W, Izzo JG, Lang J-Y, et al. The crosstalk of mTOR/S6K1 and
601 Hedgehog pathways. Cancer Cell. 20 de marzo de 2012;21(3):374-87.

602 45. Glasson SS, Blanchet TJ, Morris EA. The surgical destabilization of the medial meniscus
603 (DMM) model of osteoarthritis in the 129/SvEv mouse. Osteoarthritis and Cartilage.
604 septiembre de 2007;15(9):1061-9.

605 46. Pacheco M, Valencia M, Caparrós-Martín JA, Mulero F, Goodship JA, Ruiz-Perez VL. Evc
606 works in chondrocytes and osteoblasts to regulate multiple aspects of growth plate
607 development in the appendicular skeleton and cranial base. Bone. enero de
608 2012;50(1):28-41.

609 47. Tao F, Jiang T, Tao H, Cao H, Xiang W. Primary cilia: Versatile regulator in cartilage
610 development. Cell Prolif. marzo de 2020;53(3):e12765.

611 48. McGlashan SR, Cluett EC, Jensen CG, Poole CA. Primary cilia in osteoarthritic
612 chondrocytes: from chondrons to clusters. Dev Dyn. agosto de 2008;237(8):2013-20.

613 49. Thompson CL, Chapple JP, Knight MM. Primary cilia disassembly down-regulates
614 mechanosensitive hedgehog signalling: a feedback mechanism controlling ADAMTS-5
615 expression in chondrocytes. Osteoarthritis Cartilage. marzo de 2014;22(3):490-8.

616 50. Chang C-F, Ramaswamy G, Serra R. Depletion of primary cilia in articular chondrocytes
617 results in reduced Gli3 repressor to activator ratio, increased Hedgehog signaling, and
618 symptoms of early osteoarthritis. Osteoarthritis Cartilage. febrero de 2012;20(2):152-61.

619 51. Potocki L, Abuelo DN, Oyer CE. Cardiac malformation in two infants with
620 hypochondrogenesis. Am J Med Genet. 20 de noviembre de 1995;59(3):295-9.

621 52. Muscatello LV, Benazzi C, Dittmer KE, Thompson KG, Murgiano L, Drögemüller C, et al.
622 Ellis-van Creveld Syndrome in Grey Alpine Cattle: Morphologic, Immunophenotypic, and
623 Molecular Characterization. Vet Pathol. septiembre de 2015;52(5):957-66.

624 53. Thompson CL, Patel R, Kelly T-AN, Wann AKT, Hung CT, Chapple JP, et al. Hedgehog
625 signalling does not stimulate cartilage catabolism and is inhibited by Interleukin-1β.
626 Arthritis Res Ther. 24 de diciembre de 2015;17:373.

627 54. Lee JJ, Rothenberg ME, Seeley ES, Zimdahl B, Kawano S, Lu W-J, et al. Control of
628 inflammation by stromal Hedgehog pathway activation restrains colitis. Proc Natl Acad
629 Sci U S A. 22 de noviembre de 2016;113(47):E7545-53.

630 55. Zhou X, Liu Z, Jang F, Xiang C, Li Y, He Y. Autocrine Sonic hedgehog attenuates
631 inflammation in cerulein-induced acute pancreatitis in mice via upregulation of IL-10.
632 PLoS One. 2012;7(8):e44121.

633 56. Pérez-baos S, Gratal P, Barrasa JI, Lamuedra A, Sánchez-pernaute O, Herrero-beaumont
634 G, et al. Inhibition of pSTAT1 by tofacitinib accounts for the early improvement of
635 experimental chronic synovitis. 2019;2:1-10.

636 57. Tardio L, Andrés-Bergós J, Zachara NE, Larrañaga-Vera A, Rodriguez-Villar C, Herrero-
637 Beaumont G, et al. O-linked N-acetylglucosamine (O-GlcNAc) protein modification is
638 increased in the cartilage of patients with knee osteoarthritis. Osteoarthritis and
639 Cartilage. 2014;

640 58. Larrañaga-Vera A, Lamuedra A, Pérez-Baos S, Prieto-Potin I, Peña L, Herrero-Beaumont G,
641 et al. Increased synovial lipodystrophy induced by high fat diet aggravates synovitis in
642 experimental osteoarthritis. Arthritis Research and Therapy. 2017;19(1):264.

643 59. Villalvilla A, Gomez R, Lugo L, Lopez-Oliva F, Largo R, Herrero-Beaumont G. Aromatase
644 expression in human chondrocytes: An induction due to culture. Maturitas. 2016;85:27-
645 33.

646 60. Mediero A, Wilder T, Ramkhelawon B, Moore KJ, Cronstein BN. Netrin-1 and its receptor
647 Unc5b are novel targets for the treatment of inflammatory arthritis. FASEB Journal.
648 2016;30(11):3835-44.

649 61. Faul F, Erdfelder E, Lang A-G, Buchner A. G * Power 3 : A flexible statistical power analysis
650 program for the social , behavioral , and biomedical sciences. Behavior Research
651 Methods. 2007;39(2):175-91.

652

653 **FIGURE LEGENDS**

654 **Figure 1. Gene expression of Hedgehog (Hh) mediators in the OA *Evc*^{cKO} model and cartilage**
655 **structure.** Gene expression of *Ptch1* (A), *Gli1* (B), *Evc* (C) and *Ihh* (D) in the knees of NO-WT,
656 DMM-WT and DMM-*Evc*^{cKO} mice. Data are represented as the individual measurements of each
657 joint and expressed as mean ± SEM (NO-WT n≥7; DMM-WT n≥7; DMM-*Evc*^{cKO} n≥7).

658

659 **Figure 2. Metalloproteinases (MMP) protein levels in mouse knee joints.** Protein levels of
660 MMP-13 (A), MMP-1 (B) and MMP-3 (C) in the knees of NO-WT, DMM-WT and DMM-*Evc*^{cKO}
661 mice and their representative western blots (D,E,F). Gene expression of *Col2a1* (G) and *Agg*
662 (H), in the knees of NO-WT, DMM-WT and DMM-*Evc*^{cKO} mice. Data are represented as the
663 individual measurements of each joint and expressed as mean ± SEM (NO-WT n≥7; DMM-WT
664 n≥7; DMM-*Evc*^{cKO} n≥7).

Figure 3. Effect of *Evc* deletion on OA-associated chondrocyte hypertrophy *in vivo*. Gene expression of chondrocyte hypertrophic markers *Runx2* (A), *Col10a1* (B), *Mmp13* (C) and *Adamts5* (D), *Alpl* (E) and *Sp7* (F) in the knees of NO-WT, DMM-WT and DMM-*Evc*^{cKO} mice. Representative femur cartilage sections stained with Hematoxylin/Eosin (G). Cartilage thickness in femur calcified cartilage of NO-WT, DMM-WT and DMM-*Evc*^{cKO} mice (H). Data are represented as the individual measurements of each joint and expressed as mean ± SEM (NO-WT n≥7; DMM-WT n≥7; DMM-*Evc*^{cKO} n≥7).

Figure 4. Co-localization of hypertrophic and inflammatory markers in human cartilage. Immunofluorescence of IHH (A) and cyclooxygenase-2 (COX-2) (B), chondrocyte nuclei staining with DAPI (C)and merge (D) in human OA cartilage samples.

Figure 5. Inflammatory effect of IL-1 beta on human OA chondrocytes *in vitro*. Gene expression of Hh signaling mediators *PTCH1* (A), *EVC* (B), *GLI1* (C) and *IHH* (D) and proinflammatory mediators *IL1B* (E), *MMP13* (F), prostaglandin G/H synthase 2 (*PTGS2)* (G), prostaglandin E2 receptor (*PTGER2*) (H), *IL6* (I), inducible nitric oxide synthase (*NOS2*) (J) and monocyte chemoattractant protein-1 (*CCL2*) (K) in human OA chondrocytes treated with IL-1 beta and CPA, or vehicle (DMSO), for 24 hours. Data are normalized by chondrocytes in basal conditions (no IL-1 beta, no CPA stimulation) and expressed as mean ± SEM (n=5 independent experiments).

Supplementary Figure 1. *Evc* mRNA levels in tissues of WT, *Evc*$^{flox/-}$ and *Evc*^{cKO} animals. *Evc* gene expression in lung (A), heart (B), brain (C), muscle (D) and bone (E) of WT, *Evc*$^{flox/-}$ and *Evc*^{cKO} mice. Data are normalized with respect to *Evc* mRNA levels in WT mice and expressed as mean ± SEM (WT n=6; *Evc*$^{flox/-}$ n = 6; *Evc*^{cKO} n≥3 for lung, brain, muscle and heart; WT n=1; *Evc*$^{flox/-}$ n = 1; *Evc*^{cKO} n = 1 for bone – pool of tibiae –).

Table 1. Histopathological cartilage score in mouse knee joints. OARSI score in NO-WT, DMM-WT and DMM-*Evc*^{cKO} mouse knee joints. Data are expressed as mean ± SEM (NO-WT n=10; DMM-WT n=11; DMM-*Evc*^{cKO} n=11).*p<0.05 vs NO-WT, $^{\#}$p<0.05 vs DMM-WT.

Figure 1

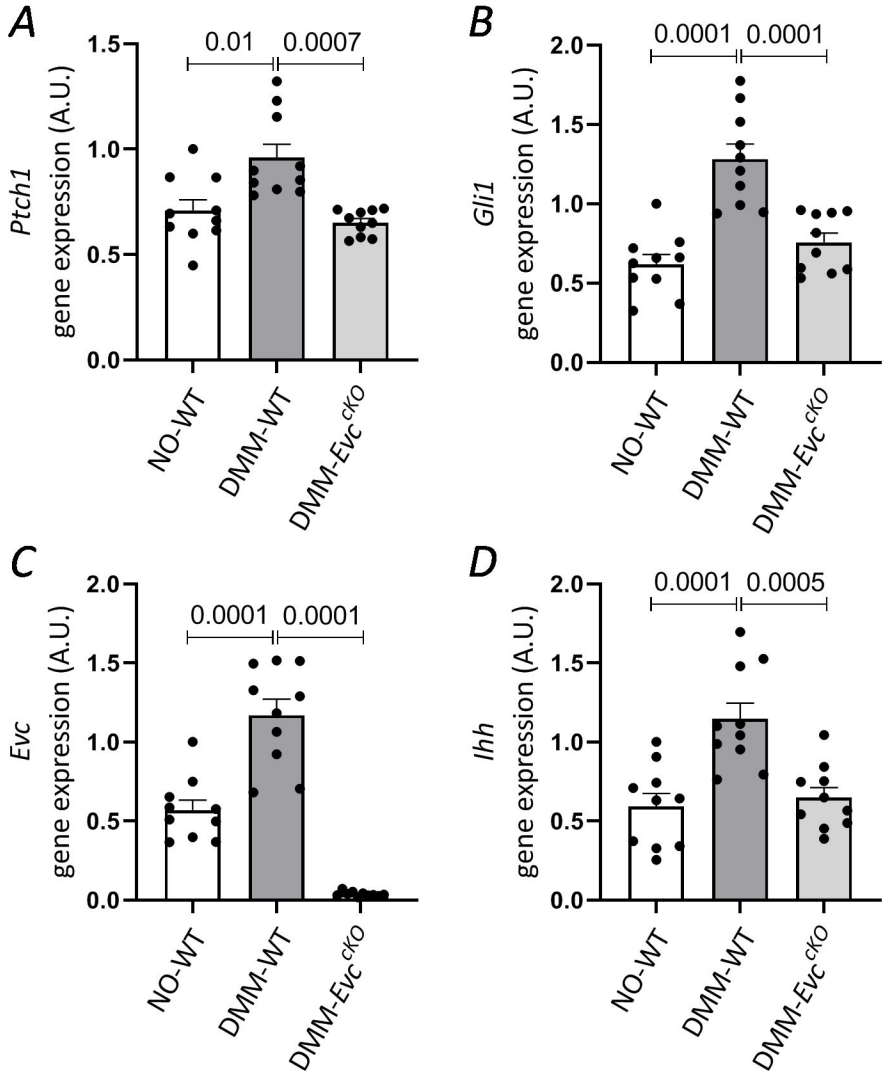
A
Ptch1
gene expression (A.U.)
0.01
0.0007
B
Gli1
gene expression (A.U.)
0.0001
0.0001
C
Evc
gene expression (A.U.)
0.0001
0.0001
D
Ihh
gene expression (A.U.)
0.0001
0.0005
NO-WT
DMM-WT
DMM-Evc cKO

Figure 2

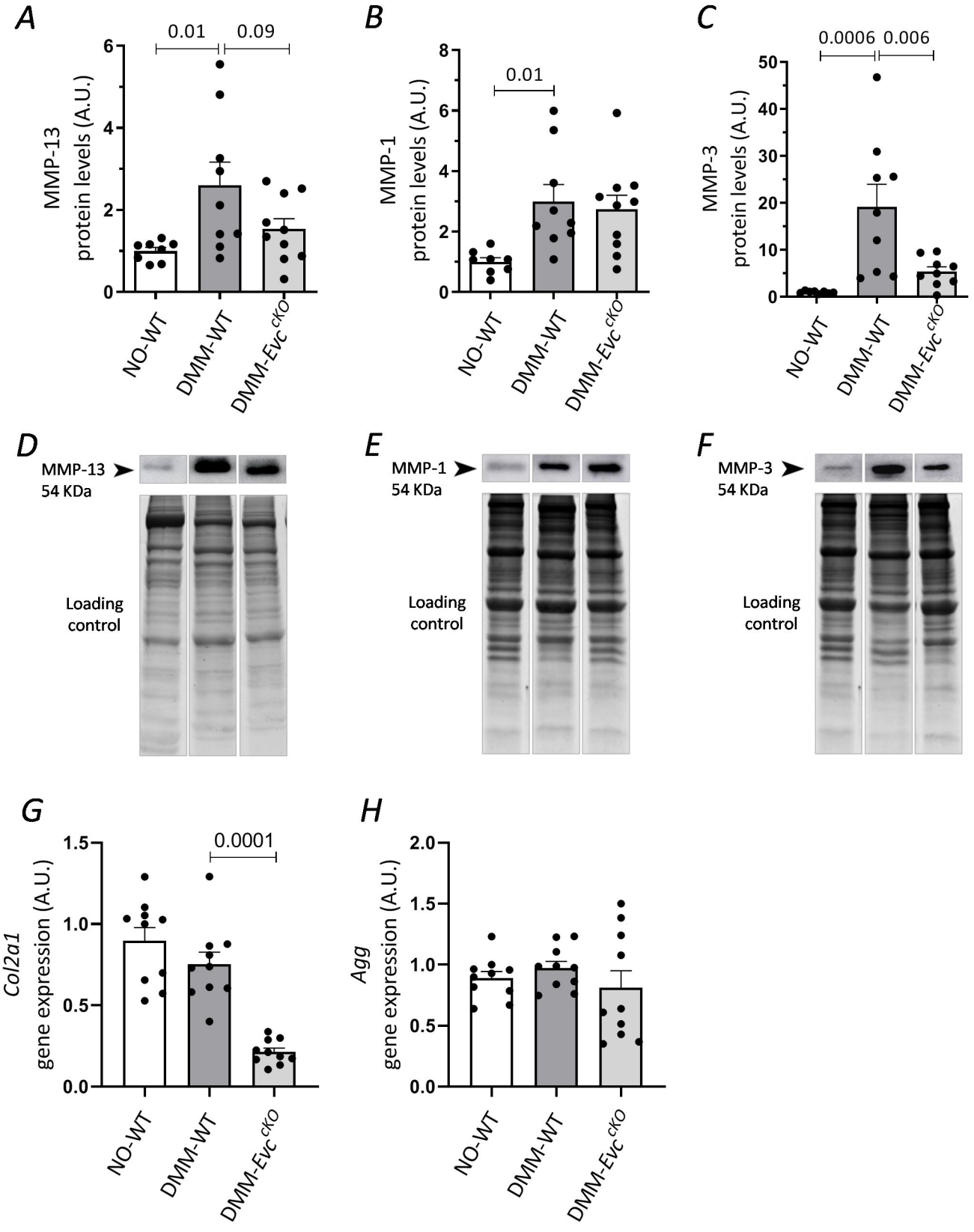
A
MMP-13 protein levels (A.U.)
0.01
0.09
NO-WT
DMM-WT
DMM-Evc cKO
B
MMP-1 protein levels (A.U.)
0.01
C
MMP-3 protein levels (A.U.)
0.0006
0.006
D
MMP-13
54 KDa
Loading control
E
MMP-1
54 KDa
F
MMP-3
54 KDa
G
Col2a1 gene expression (A.U.)
0.0001
H
Agg gene expression (A.U.)

Figure 3

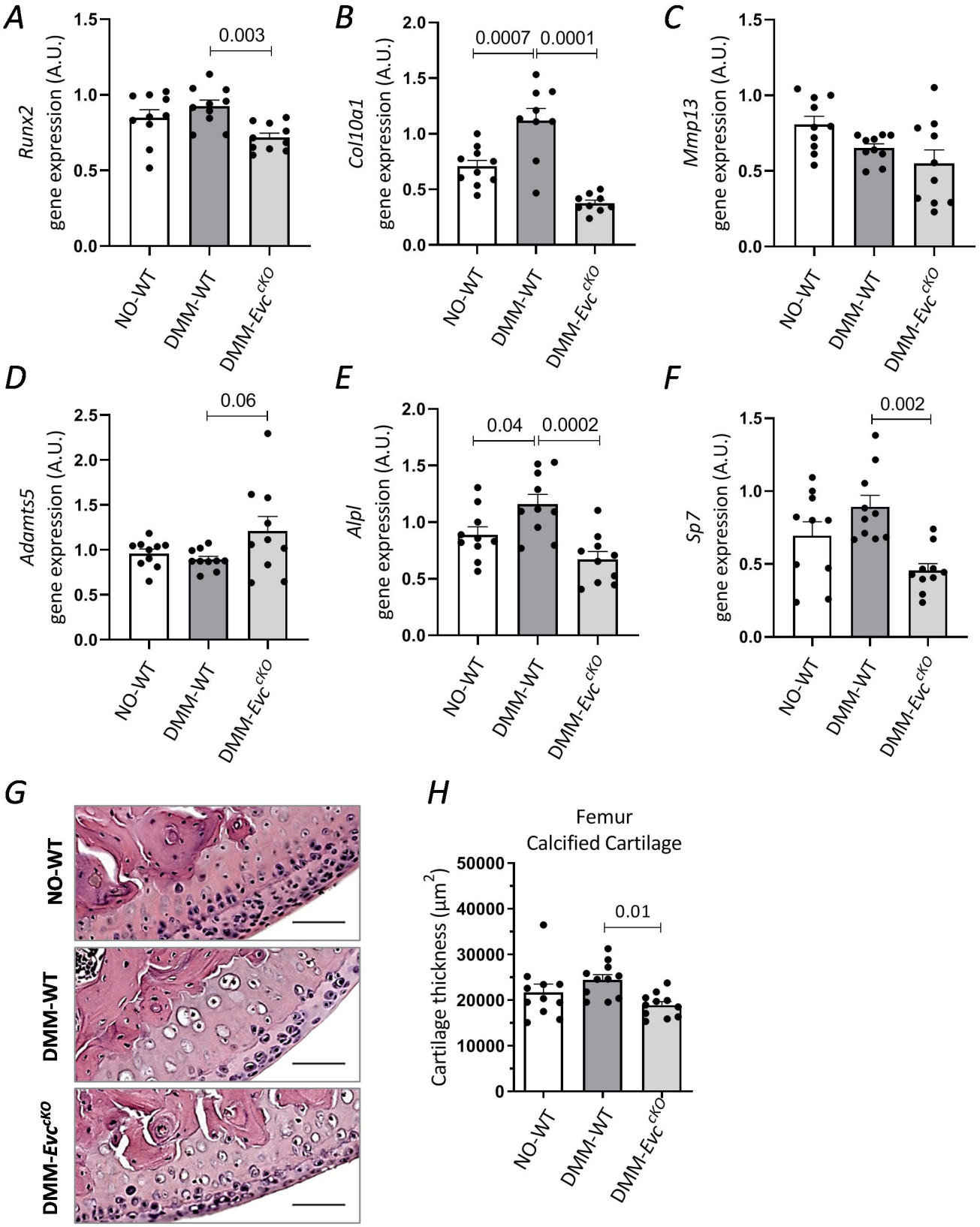
A
Runx2
gene expression (A.U.)
0.003
B
Col10a1
gene expression (A.U.)
0.0007
0.0001
C
Mmp13
gene expression (A.U.)
D
Adamts5
gene expression (A.U.)
0.06
E
Alpl
gene expression (A.U.)
0.04
0.0002
F
Sp7
gene expression (A.U.)
0.002
NO-WT
DMM-WT
DMM-Evc cKO
G
NO-WT
DMM-WT
DMM-Evc cKO
H
Femur
Calcified Cartilage
Cartilage thickness (μm2)
0.01

Figure 4

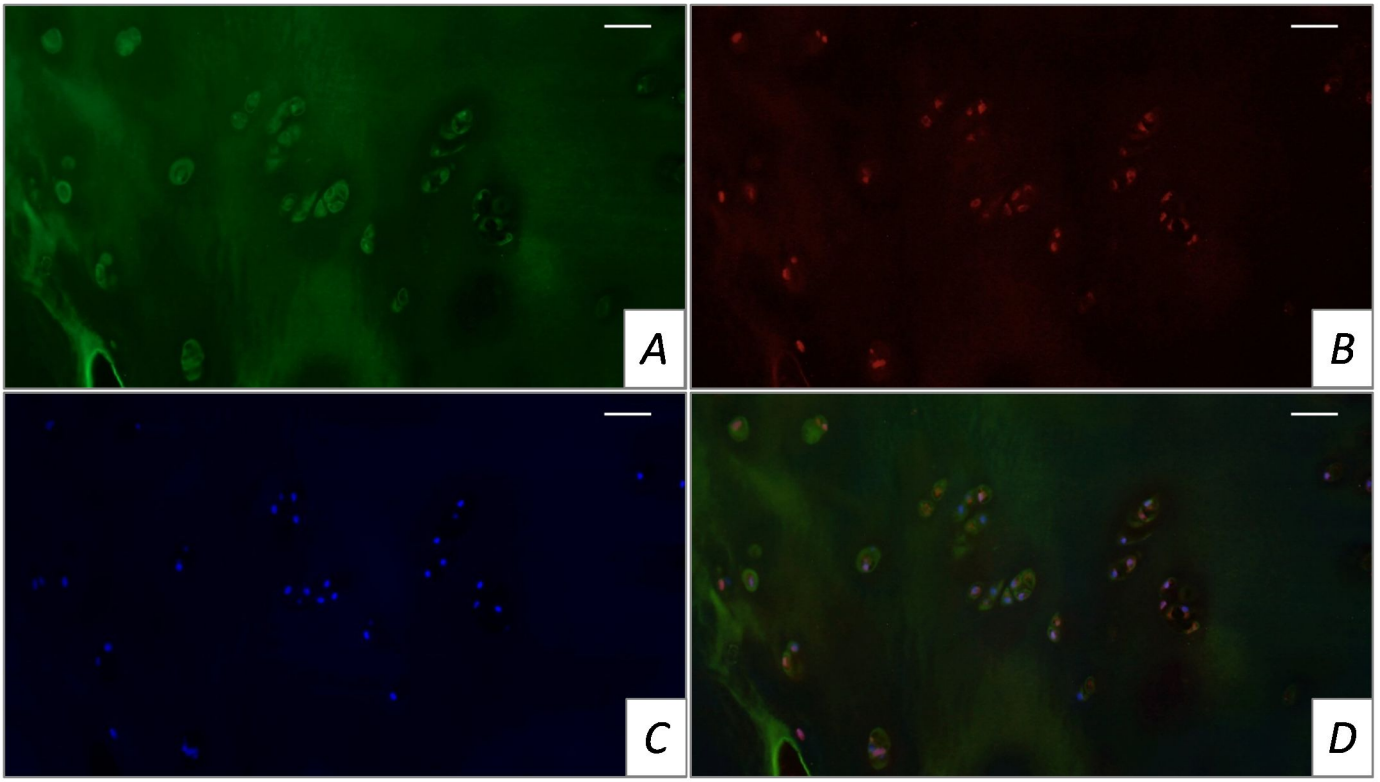

Figure 5

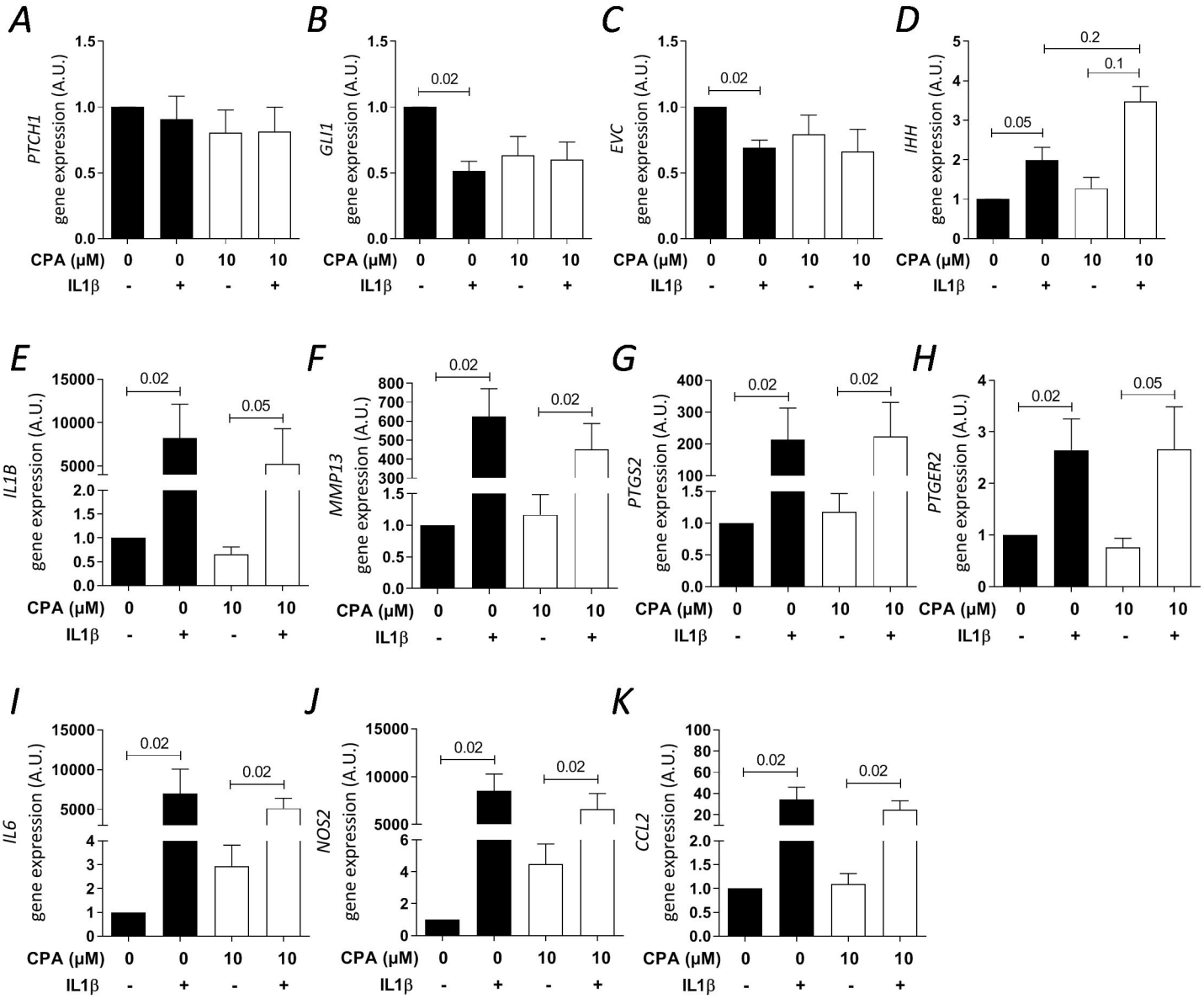
A
PTCH1
gene expression (A.U.)
B
GLI1
0.02
C
EVC
0.02
D
IHH
0.2
0.1
0.05
E
IL1B
0.02
0.05
F
MMP13
0.02
0.02
G
PTGS2
0.02
0.02
H
PTGER2
0.02
0.05
I
IL6
0.02
0.02
J
NOS2
0.02
0.02
K
CCL2
0.02
0.02
CPA (μM) 0 0 10 10
IL1β - + - +

Supplementary Figure 1

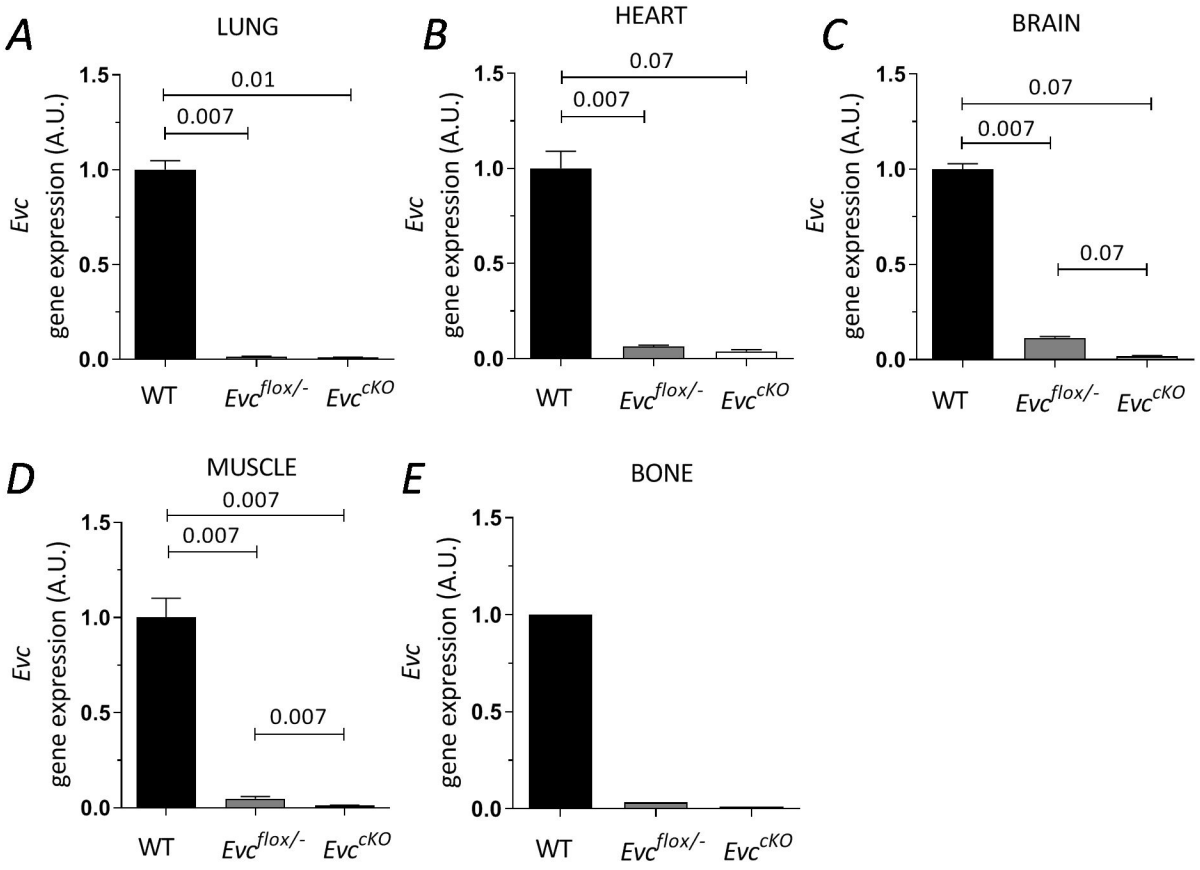

Table 1

Table 1 Histopathological score in mouse knee joints

Group	NO-WT	DMM-WT	DMM-*Evc*^{cKO}
OARSI Score (SEM)	1.15 (0.198)	2.818 (0.615)*	2.727 (0.718)